Ageing phenomena identification of PEMFC using the DRT tool

Laurine TURPIN[a,b], Quentin CACCIUTTOLO[a], Boyang XU[a], Zhixue ZHENG[b], Marie-Cécile PÉRA[b]
[a] IFP Energies nouvelles, Rond-point de l'échangeur de Solaize, BP3, 69390 Solaize, France
[b] Université Marie et Louis Pasteur, CNRS, Institut FEMTO-ST, FCLAB, F-90000, Belfort, France

ABSTRACT - This study utilizes the Electrochemical Impedance Spectroscopy (EIS) and the Distribution of Relaxation Times (DRT) to analyse the aging of Proton Exchange Membrane Fuel Cells (PEMFC). It aims to understand the underlying degradation mechanisms to enhance the efficiency and durability of PEMFC in heavy-duty vehicle applications. The DRT method applied on an aging stack dataset provides in-depth insights into specific degradation processes, such as the gas diffusion layer efficiency (GDL) and catalyst corrosion, through detailed impedance spectra analysis. Preliminary results indicate that DRT has the potential to improve ageing models. Future research will focus on applying this method to additional experimental datasets, while considering various operational conditions that impact degradation.

Keywords—PEMFC, Electrochemical Impedance Spectroscopy, Equivalent Circuit Modelling, Distribution of Relaxation Times

1. INTRODUCTION

Hydrogen systems are foreseen to be highly promising devices to store energy. Especially, Fuel Cells (FC) could be a key technology to enhance the sustainable energy transition, when fed with decarbonized dihydrogen.

Among fuel cells, ones of interest due to their compacity, high-energy density and low temperature are Proton Exchange Membrane (PEM) Fuel Cells. They could suit needs for various application, heavy-duty vehicles for instance.

However, further investigations still remain to be done to improve their efficiency and durability before they can be widely commercialized.

A PEM fuel cell, although its main reaction is simple, converting hydrogen and oxygen into water, electricity and heat (1), is a very complex system. Its core is called the Membrane Electrode Assembly (MEA) and is composed of Gaz Diffusion Layers (GDL), Catalyst Layers (CL) and the electrolyte membrane. Around the MEA are two Bipolar Plates (BP) to feed the cell with gases, extract the water produced and connect the cell electrically and gaskets to avoid leakages. To have more power, these cells are assembled in series to build a stack. The coolant, air or deionized water, flows in between head-to-head bipolar plates.

$$H_2 + \frac{1}{2}O_2 \rightarrow H_2O + electricty + heat \qquad (1)$$

The degradation of a PEMFC is often looked through the evolution of its polarization curve, the power or the potential at nominal current. The model resulting of this polarization curve commonly considers only macroscopic activation losses linked to electrochemical kinetics, ohmic losses related to proton and electron conductivity respectively in the membrane and in GDL and BP, and concentration losses representing gas transport through the GDL. However, the evolution of these losses cannot always be directly and precisely related to a single ageing phenomenon but can rather be a higher scale indicator.

As the research on modelling PEMFC ageing behaviour is still on-going, with specificity for each stack, new tools allow us to get a better understanding of the ageing phenomena overcoming the limitations of what the polarization curve could show. Hence, by applying that knowledge to ageing models, the state of health evolution prediction of the PEMFC could be improved.

This work focuses on using the Distribution of Relaxation Times (DRT) on experimental electrochemical impedance spectroscopy (EIS) to separately identify the importance of each degradation phenomenon. More and more studies are turning to EIS and DRT analysis for fuel cells [20, 21]. The tools are used for different technologies from PEMFC to SOFC but mainly on single cells. Fewer studies on stacks can be found, and they are primarily focused on the impact of operating conditions on the EIS/DRT spectra rather than on applying this method to ageing data [5, 18].

Therefore, this study proposes one of the first approaches to using DRT on EIS measurements obtained from a PEMFC short-stack under experimental conditions. It presents a thorough analysis of the methodology to assess the DRT results in a robust and meaningful way.

2. DEGRADATION PHENOMENA

Among the many ways to study the ageing of PEMFC, this study presents the main contributing phenomena [1] by a component-by-component analysis.

2.1. Membrane

The membrane allows protons to transfer from the anode to the cathode. A common material used is Nafion™ that is composed of polyfluorosulfonic acid (PFSA) with hydrophobic chain of polytetrafluoroethylene (PTFE) to deal with water management and hydrophilic chain for the proton transport.

However, this structure can be deteriorated due to O_2 permeation, which create hydrogen peroxide H_2O_2 at the electrodes, ultimately degrading the polymer structure of the membrane. Additionally, the structure can be poisoned by multivalent cations (Fe^{3+}, Al^{3+}, etc.). The migration of platinum (Pt) in the membrane creating a Pt band also has a significant impact [14, 22].

Furthermore, the membrane is subjected to heavy mechanical stresses due to the sealing requirements, which

intensify when the membrane becomes hydrated and expands, leading to increased mechanical and thermal strain.

All these phenomena can reduce the conductivity, create pinholes, and can be enhanced by other deterioration issues.

2.2. Catalytic Layer (CL)

The electrochemical reactions occur at the triple points in the CL. The triple points are active spots where the electrons, the protons and the gases (H_2/O_2) all come together. To do this, Pt nanoparticles are applied on a layer of active carbon, which conducts the electrons. Meanwhile, this layer is surrounded by an ionomer to facilitate the diffusion of cations.

The main degradation factor is probably the alteration of Pt. First, we observe that Pt particles tend to agglomerate in bigger structures, known as Ostwald ripening, that reduces the catalytic surface/volume ratio. The Pt oxidation and precipitation with H_2 into the membrane can create the Pt band explained in 2.1. Moreover, the carbon layer can be corroded by O_2 molecules, leading to more Pt structure detaching. The Pt can also be poisoned by CO, SO_2, NO, NH_3, etc., which reduces the Electrochemical Surface Area (ECSA), thereby reducing the efficiency as less species can react [15].

2.3. Gas Diffusion Layer (GDL) and Bipolar Plates (BP)

The GDL is mainly impacted by the carbon corrosion, which changes its microstructure and impacts its transport properties. When combined with the loss of PTFE, the GDL becomes less hydrophobic and the probability of water flooding increases [16].

The corrosion of bipolar plates increases their ohmic resistance, leading to a decline in the output voltage. This can also lead to the membrane poisoning by cations, as described in 2.1 [17].

By understanding all these interdependent degradation phenomena, it becomes clear that the system is complex as they are all intricately linked, and one can cause chain reactions that will propagate through the different layers.

3. ANALYSIS TOOLS

EIS is a very useful tool to study the electrochemical properties of a system and decouple phenomena with different dynamics. By measuring the magnitude and phase response to a small amplitude voltage or current perturbation over a range of frequencies, an impedance spectrum is generated, as shown in Fig. 1.

It can be expected that changes in key parameters such as the ohmic resistance R_0 or the capacitance of the PEMFC can be observed through the evolution of the impedance spectrum.

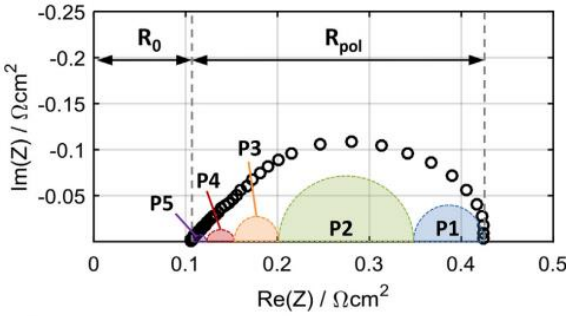

Fig. 1. EIS spectrum indicating the Ohmic and Polarization resistances and the peaks associated in the DRT [2].

Various analytical methods can then be used to interpret these changes and reveal the underlying degradation mechanisms.

3.1. Equivalent Circuit Modelling (ECM)

The ECM involves fitting the impedance spectrum using an electrical circuit. The main components used are often a resistor to represent the ohmic resistance, RC circuits for the reaction kinetics, and an infinite Warburg element for the mass transport loss at the cathode.

However, the limitations of the ECM method reside in the simplification of the system, the need for an *a priori* model, the parameter determination that can be tricky due to the non-linearities and sometimes an equivalent circuit could have a good fitting whilst having no physical meaning. Moreover, the fitting process can be tedious and can be difficult to automate.

3.2. Distribution of Relaxation Times (DRT)

On the other hand, the DRT method, a mathematical tool, offers deeper insights into the individual contribution of various phenomena to the impedance spectra. The DRT produces a distribution of time constants, $g(\tau)$, associated with an equivalent series of parallel RC circuits (2).

$$Z(\omega) = R_0 + R_{pol}\int_0^{\infty} \frac{g(\tau)}{1+j\omega\tau} d\tau \qquad (2)$$

Where R_0 is the ohmic resistance and R_{pol} is the polarization resistance that can be read on the impedance spectra (Fig. 1). A time constant $\tau = RC$ is associated to each RC circuit. For discrete calculation, one can typically use an equally spaced logarithmic time constants giving (3).

$$Z(\omega) = R_0 + R_{pol}\sum_{k=1}^{N} \frac{g_k}{1+j\omega\tau_k} \qquad (3)$$

Heinzmann *et al.* [2] have shown in a highly controlled environment and on a single cell that the resulting graph reveals five distinct peaks associated with smaller scale phenomenon such as gas diffusion or Oxygen Reduction Reaction (ORR) hence the kinetics of the reaction (Fig. 2).

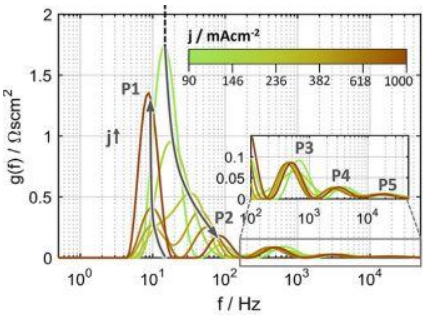

Fig. 2. DRT results for high current densities with 70% Relative Humidity (RH), and T = 80°C [2].

By studying how these peaks evolve under different parameters, we could improve our understanding on how these phenomena affect ageing.

4. RESULTS

4.1. Database

The database used for this study is collected from the IEEE PHM 2014 data challenge [3]. The 5-cell short stack FC2 was operated under rippled current at ± 10% of the nominal current density within the frequency range of 0.05 Hz to 10 kHz. In

particular, the EIS measurements performed under the different current densities 0.2, 0.45 and 0.7 A·cm^{-2} at t = [0, 35, 182, 343, 515, 666, 830, 1016] h during the ageing test are considered. In Fig. 3, the evolution of the polarization curves through time shows the impact of ageing hence enforcing that this database is suitable for our work.

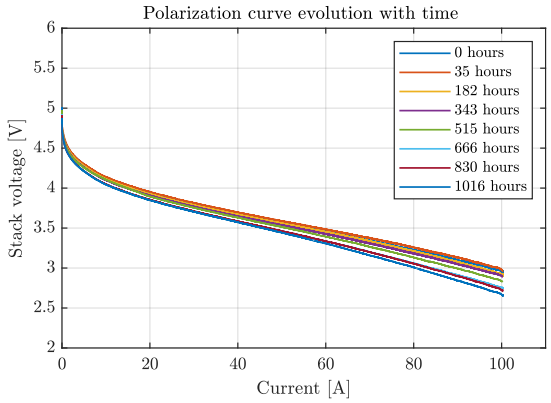

Fig. 3. Polarization Curves evolution with time.

The Kramers-Kronig test (KK-test) [6, 7, 8] was performed on the database to evaluate the quality of the EIS measurements. A tolerance for the deviation of 1% for the residuals was considered, and only one outlier was removed and replaced by the fitted value to keep the information.

4.2. Study

The analysis performed for this work consider first the parameter sensitivity analysis on the used DRT tool and second the application of DRT on ageing data.

The DRT tool developed in [11, 12] proposes various settings depending on the approach and data under study.

The main parameters are the discretization methods (Table 1), regularization functions which are mainly Radial Basis Functions (RBF), the type of run (simple or Bayesian [9, 10]) and the RBF shape factor control. To determine the set of parameters with the best results, one can consider the following criteria:

- **CI**: When performing Bayesian Runs, a Credibility Interval (CI) of 99% is obtained for the DRT. It is linked to the used discretisation method. It is considered small when $\frac{\Delta\gamma}{\gamma} = \frac{|\gamma_{peak} - \gamma_{CI}|}{\gamma_{peak}} \leq 15\%$ on the second peak (e.g., Fig. 4.c), large when $\frac{\Delta\gamma}{\gamma} \geq 100\%$ (e.g., Fig. 5.a) and medium when $15\% < \frac{\Delta\gamma}{\gamma} < 100\%$.
- **NbS**: The readability of the peak's amplitude which is related to the number of samples for a Bayesian run.
- **NbP**: The number of peaks (without extrapolating too much) which depends on the shape factor control.
- **Fit**: The fitting of the EIS measurements for which the residuals can be a good indicator on the precision. It is considered very good when the residuals are in the range $\pm 1 \times 10^{-4}$ for the frequency range 10 Hz to 100 Hz without too many oscillations. It is good when it stays in the range $\pm 2 \times 10^{-4}$ in this given range. Only this range is considered as the residuals for the rest of the frequencies do not present a significant and measurable difference.
- **FR**: The frequency range which depends on the discretization method and the measurements performed. It is real when only considering the actual measurements from 0.05 Hz to 10 kHz and extended when there is an extrapolation giving a frequency range between 0.02 Hz and 30 kHz.
- **ExeT**: The execution time which depends on the discretization method. It will be considered very fast when taking less than 30 s, medium when taking between 30 s and 2 min and slow if the processing time exceeds 2 min. This criterion's results are highly correlated to the used computer.

Table 1. RBF discretization functions available in the DRT tool [13].

Function	Expression
Gaussian (G)	$\exp(-(\mu x)^2)$
C^2 Matérn (C2M)	$\exp(-\lvert\mu x\rvert)(1+\lvert\mu x\rvert)$
C^4 Matérn (C4M)	$\exp(-\lvert\mu x\rvert)(1+\lvert\mu x\rvert+\frac{1}{3}\lvert\mu x\rvert^2)$
C^6 Matérn (C6M)	$\exp(-\lvert\mu x\rvert)(1+\lvert\mu x\rvert+\frac{2}{5}\lvert\mu x\rvert^2+\frac{1}{15}\lvert\mu x\rvert^3)$
Inverse Quadratic (IQa)	$\frac{1}{1+(\mu x)^2}$
Inverse Quadric (IQb)	$\frac{1}{\sqrt{1+(\mu x)^2}}$
Cauchy (C)	$\frac{1}{1+\lvert\mu x\rvert}$
Piecewise Linear (PL)	$\begin{cases} 1-\frac{\ln\tau-\ln\tau_m}{\ln\tau_{m-1}-\ln\tau_m} & \tau_{m-1}\leq\tau\leq\tau_m \\ 1-\frac{\ln\tau-\ln\tau_m}{\ln\tau_{m+1}-\ln\tau_m} & \tau_m\leq\tau\leq\tau_{m+1} \\ 0 & \tau<\tau_{m-1}\ or\ \tau_{m+1}<\tau \end{cases}$

With $x = |\ln\tau - \ln\tau_m|$ and μ is the shape-factor of the RBF

The different settings were applied to the database presented in section 4.1.

4.3. Results

4.3.1. Parameter sensitivity analysis

The first presented result considers the sensitivity analysis study conducted on the data to see which set of parameters should be used for this work.

Table 2. Comparison between discretization functions.

	CI	NbP	Fit	FR	ExeT
At 0.2 A·cm^{-2}					
G	Large	4	Very Good	Extended	Medium
C2M	Large	4	Very Good	Extended	Medium
C4M	Medium	3	Good	Extended	Medium
IQa	Large	4	Very Good	Extended	Slow
PL	Small	3	Very good	Real	Very fast
At 0.45 A·cm^{-2}					
G	Large	4	Good	Extended	Medium
C2M	Large	4	Good	Extended	Medium
C4M	Medium	3	Good	Extended	Medium
IQa	Large	4	Good	Extended	Slow
PL	Small	3	Good	Real	Very fast
At 0.7 A·cm^{-2}					
G	Large	4	Very Good	Extended	Medium
C2M	Large	4	Very Good	Extended	Medium
C4M	Medium	3	Good	Extended	Medium
IQa	Large	3	Good	Extended	Slow
PL	Small	2	Very Good	Real	Very fast

The study has shown that the results were invariant to the regularization method. It was chosen arbitrarily to use the Generalized Cross-Validation (GCV) method throughout the whole study. Also, the fitting was always done using an inductance component to model the inductive loss from measurements.

The Full Width Half Maximum coefficient (FWHM) was adjusted to avoid overfitting (appearance of oscillations) between 0.4 and 0.7. The number of samples (NbS) for the Bayesian run was set to 2500 after testing several other quantities because it was a good trade-off between the peaks' maximum readability and the computation time. Bayesian runs were performed to get more information on the validity of the graph, the associated uncertainty and how to exploit it.

Regarding the discretization functions, one can discard the C^6 Matérn, the Inverse Quadric and the Cauchy methods, which give unexploitable results because the EIS data fitting optimization could not converge to an acceptable solution.

The comparison of the other methods is given in Table 2 with the criteria detailed in section 4.2.

This shows that the piecewise linear has the most exploitable results, especially considering the CI criteria, and has a high computational efficiency compared to the other methods. However, it is limited to the measured frequency range and

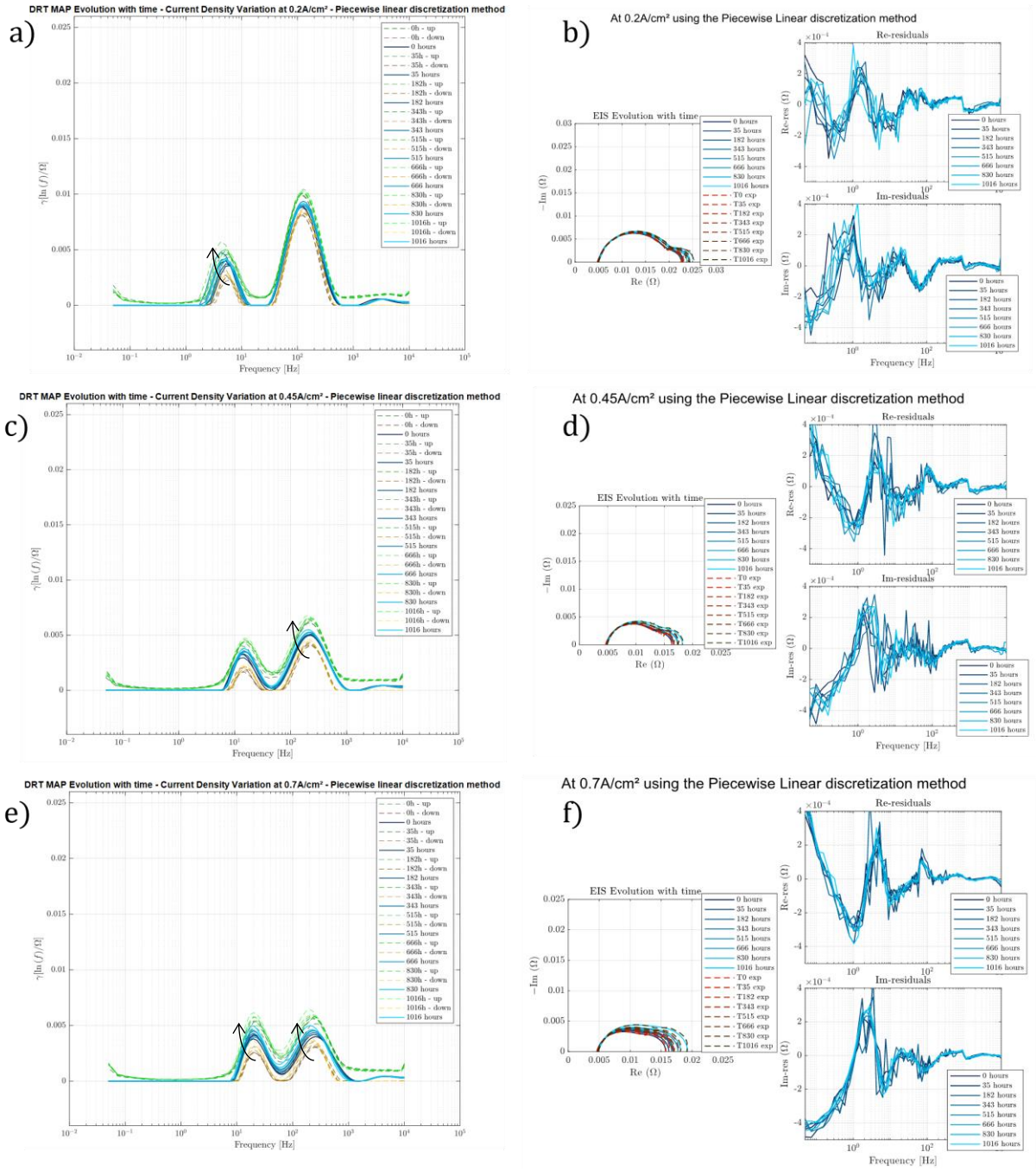

Fig. 4. Bayesian run; Piecewise Linear - DRT MAP evolution over time with current densities of a) 0.2 A·cm^{-2}, c) 0.45 A·cm^{-2} and e) 0.7 A·cm^{-2}. relative EIS fitted spectra b) 0.2 A·cm^{-2}, d) 0.45 A·cm^{-2} and f) 0.7 A·cm^{-2}.

cannot extrapolate to a larger frequency range contrarily to the other methods. Finally, fewer peaks are observed compared to the Gaussian method, which can pose limitations for further studies. Moreover, the Gaussian method shows a large CI which makes the interpretation of the results more difficult as the uncertainty will be increased.

Hence, when applying the DRT method to the ageing data, a comparison will be made between the Gaussian RBF and the piecewise linear discretization methods.

4.3.2. Applying DRT to ageing data

In Fig. 4.a), 4.c) and 4.e), the evolution the Maximum-A-Posteriori (MAP) DRT spectra for the different current densities can be seen. The EIS fitting results regarding the experimental data and the residuals for both the real and imaginary parts can be seen in Fig. 4.b), 4.d) and 4.f). The DRT results for the Gaussian method are shown in Fig. 5.a), 5.c) and 5.e), and EIS results in Fig. 5.b), 5.d) and 5.f).

For the DRTs, the peaks are shifted to higher frequencies and their amplitude is reduced as the current density increases. For example, in Fig. 5, the first peak is around 5 Hz at 0.2 A·cm^{-2} and at 20 Hz at 0.7 A·cm^{-2}. It makes sense as the set point current

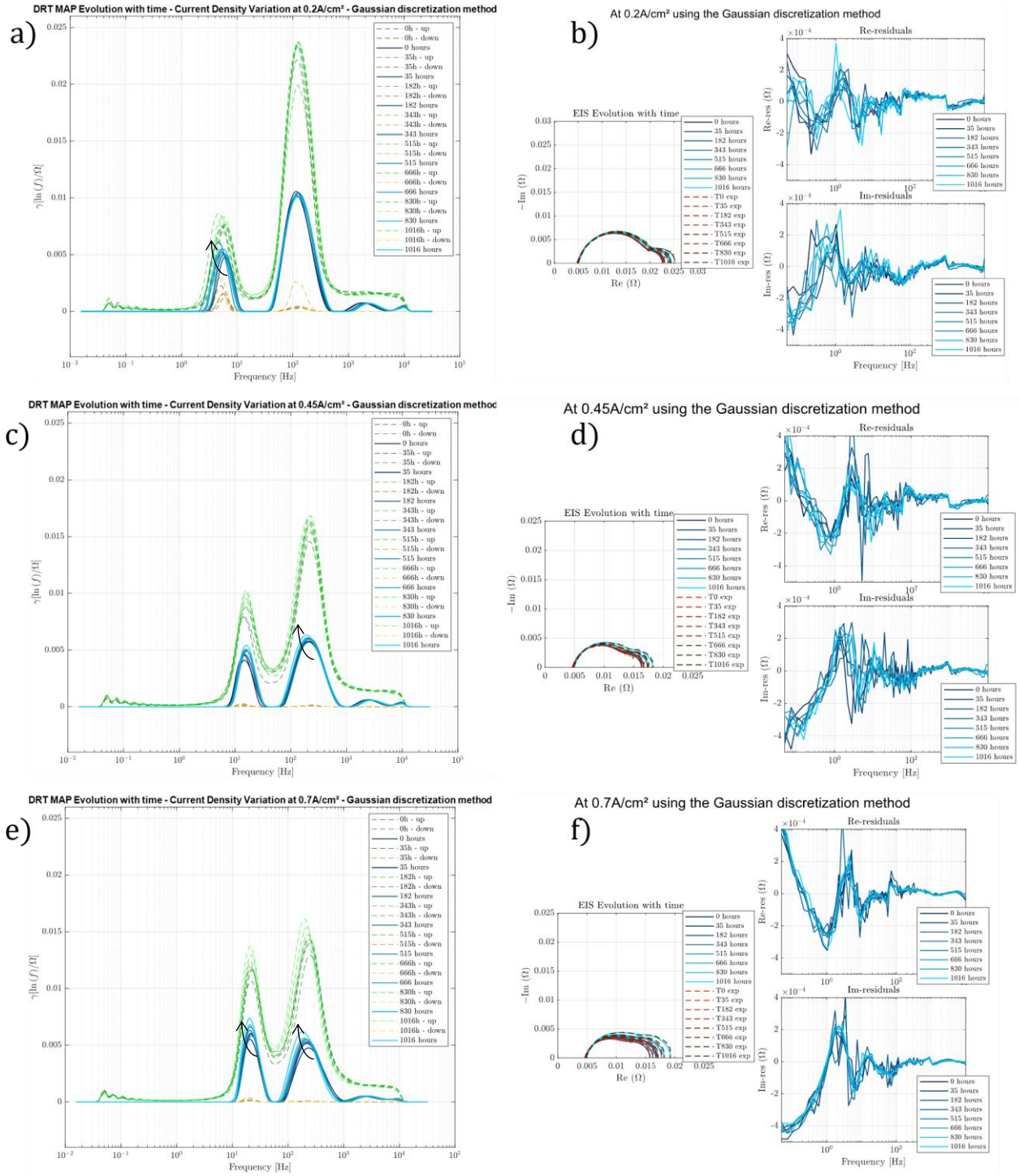

Fig. 5. Bayesian run; Gaussian - DRT MAP evolution over time with current densities of a) 0.2A·cm^{-2}, c) 0.45 A·cm^{-2} and e) 0.7 A·cm^{-2} and relative EIS fitted spectra b) 0.2A·cm^{-2}, d) 0.45 A·cm^{-2} and f) 0.7 A·cm^{-2}.

is increased, and it is logical that the phenomenon related to the reaction is increasing as it is happening faster. The shift in amplitude should be further investigated.

There is also a shift in frequency and/or amplitude when comparing MAP DRT spectra through time. Indeed, the time-evolution of the spectra suggests that the associated phenomena are slowed down. This tendency is clearly visible at higher current densities but is not as clear at lower current densities. In Fig. 5.c), at 0.7 $A \cdot cm^{-2}$:

- The first peak's amplitude is increased by 25% between t = 0 h and t = 1016 h.
- the second peak is at 250 Hz at t = 0 h and at 180 Hz at t = 1016 h and the amplitude is increased by 44%.
- The third peak is shifted in frequency from 2 kHz at t = 0 h to 2.4 kHz at t = 1016 h.

For the piecewise linear results in Fig. 4., these orders of magnitude are the same for the first two peaks.

This is interesting as Heinzmann *et al.* [2] has shown to which degradation phenomena the peaks can be related:

- The first peak can be correlated with the GDL corrosion or degradation, its evolution analysis shows that there is an increased flooding and a reduced gas diffusion to the CL.
- The second peak evolution indicates that the kinetic was reduced due to the reduction of the ECSA. This likely indicates catalyst corrosion and the occurrence of the Ostwald ripening phenomenon.

Regarding the EIS, on the contrary, the best fit to the measured data is achieved at the lower current densities. Also, the residuals are higher for the lower frequencies, which makes sense considering the measurement performed, however they are staying in a low range, which is still acceptable in the range of $\pm 4 \times 10^{-4}$.

Similar conclusions for the DRT and EIS spectra can be drawn using both discretization method. However, as stated before, the confidence in the MAP result is highly reduced for the Gaussian method as the CI goes up to twice the MAP amplitude whilst, with this method, more peaks are visible for all current densities and at all times. A trade-off is definitely needed between information and accuracy.

These conclusions are first assumptions that could be drawn and are still preliminary, but they indicate tendencies that could be exploited for future work. The data obtained could even be further studied to extract other information on the behaviour of a stack.

5. CONCLUSIONS

Our results and findings suggest that the DRT method on EIS is promising in identifying the individual contribution of degradation phenomena to the ageing of a PEMFC stack.

It is also interesting to see that we could be able to identify the parameters related to the degradation phenomena and how they evolve through time. This could be particularly interesting for phenomena that do not necessarily show up on the polarization curve.

In the future, further studies will be conducted, as an ageing test campaign is planned to apply the method to new datasets. This can be challenging as many operating conditions can affect the degradation of the stack (pressure, stoichiometry, relative humidity, …). However, these efforts could help refining the ageing models and ultimately enable their use in control algorithms to increase the durability of a stack.

6. ACKNOWLEDGEMENT

This work has been supported by the Graduate School EUR EIPHI (ANR-17-EURE-0002) and the region Bourgogne Franche-Comté.

7. REFERENCES

[1] F.A. de Bruijn *et al*., «Review: Durability and Degradation Issues of PEM Fuel Cell Components. » Fuel Cells, 8: 3-22, 2008.

[2] M. Heinzmann *et al*., «Advanced impedance study of polymer electrolyte membrane single cells by means of distribution of relaxation times», Journal of Power Sources, vol. 402, 2018, p. 24-33.

[3] E. Pahon *et al*., «Impact of current ripples on the durability of proton exchange membrane fuel cells based on two ageing datasets», Data in Brief, vol. 45, 2022.

[4] T. Wan *et al*., «Influence of the discretization methods on the distribution of relaxation times deconvolution: implementing radial basis functions with DRTtools», Electrochimica Acta, 2015, 184, 483-49.

[5] J. Zuo *et al*., Degradation root cause analysis of PEM fuel cells using distribution of relaxation times, Applied Energy, Volume 378, Part A, 2025.

[6] M. Schönleber *et al*., A Method for Improving the Robustness of linear Kramers-Kronig Validity Tests, Electrochimica Acta 131, 2014.

[7] B. A. Boukamp, J. Electrochem. Soc., 142 (1995) 1885.

[8] Tool available at : https://www.iam.kit.edu/et/english/Lin-KK.php.

[9] F. Ciucci, C. Chen, Analysis of Electrochemical Impedance Spectroscopy Data Using the Distribution of Relaxation Times: A Bayesian and Hierarchical Bayesian Approach, Electrochimica Acta, 167 (2015) 439-454.

[10] M.B. Effat, F. Ciucci, Bayesian and Hierarchical Bayesian Based Regularization for Deconvolving the Distribution of Relaxation Times from Electrochemical Impedance Spectroscopy Data, Electrochimica Acta, 247 (2017) 1117-1129.

[11] T.H. Wan *et al*., Influence of the Discretization Methods on the Distribution of Relaxation Times Deconvolution: Implementing Radial Basis Functions with DRTtools, Electrochimica Acta, 184 (2015) 483-499.

[12] A. Maradesa *et al*., Selecting the Regularization Parameter in the Distribution of Relaxation Times, Journal of the Electrochemical Society, 170 (2023) 030502.

[13] Tool available at : https://github.com/ciuccislab/pyDRTtools.

[14] P. Ren *et al*., Degradation mechanisms of proton exchange membrane fuel cell under typical automotive operating conditions, Progress in Energy and Combustion Science, Volume 80, 2020, 100859.

[15] R.E. Rosli *et al*., A review of high-temperature proton exchange membrane fuel cell (HT-PEMFC) system, International Journal of Hydrogen Energy,Volume 42, Issue 14,2017, Pages 9293-9314

[16] K-Y. Song, H-T. Kim, Effect of air purging and dry operation on durability of PEMFC under freeze/thaw cycles, International Journal of Hydrogen Energy, Volume 36, Issue 19,2011,Pages 12417-12426.

[17] M. Kumagai *et al*., Corrosion behavior of austenitic stainless steels as a function of pH for use as bipolar plates in polymer electrolyte membrane fuel cells, Electrochimica Acta, Volume 53, Issue 12, 2008.

[18] T. Reshetenko, A. Kulikovsky, Understanding the distribution of relaxation times of a low–Pt PEM fuel cell, Electrochimica Acta, Volume 391, 2021, 138954.

[19] Zhu D, Yang Y, Ma T. Evaluation the Resistance Growth of Aged Vehicular Proton Exchange Membrane Fuel Cell Stack by Distribution of Relaxation Times. *Sustainability*. 2022; 14(9):5677.

[20] H. Yuan *et al*., Quantitative analysis of internal polarization dynamics for polymer electrolyte membrane fuel cell by distribution of relaxation times of impedance, Applied Energy, Volume 303, 2021, 117640.

[21] H. Schichlein *et al*., Deconvolution of electrochemical impedance spectra for the identification of electrode reaction mechanisms in solid oxide fuel cells, Journal of Applied Electrochemistry 32, 875–882, 2002.

[22] W. Touil *et al*., "Control oriented modeling of integrated catalyst and membrane degradation in PEM fuel cells," *2024 IEEE Transportation Electrification Conference and Expo (ITEC)*, Chicago, IL, USA, 2024, pp. 1-7.